Chapter 8
Fabrication of Nanostructures with Bottom-up Approach and Their Utility in Diagnostics, Therapeutics, and Others

Sanjay Kumar, Pulak Bhushan and Shantanu Bhattacharya

Abstract Nanofabrication has been a critical area of research in the last two decades and has found wide-ranging application in improvising material properties, sensitive clinical diagnostics, and detection, improving the efficiency of electron transport processes within materials, generating high energy densities leading to pulse power, novel therapeutic mechanisms, environmental remediation and control. The continued improvements in the various fabrication technologies have led to realization of highly sensitive nanostructure-based devices. The fabrication of nanostructures is in principle carried out primarily using top-down or bottom-up approaches. This chapter summarizes the important bottom-up nanofabrication processes for realizing nanostructures and also highlights the recent research conducted in the domain of therapeutics and diagnostics.

Keywords Nanofabrication · Bottom-up approach · Diagnostics and therapeutics

Sanjay Kumar and Pulak Bhushan: Both authors have equal contribution in this chapter.

S. Kumar (✉) · P. Bhushan · S. Bhattacharya (✉)
Microsystems Fabrication Laboratory, Department of Mechanical Engineering, Indian Institute of Technology Kanpur, Kanpur, India
e-mail: sanjay21505@gmail.com

S. Bhattacharya
e-mail: bhattacs@iitk.ac.in

P. Bhushan
e-mail: pulakbhushan@gmail.com

S. Bhattacharya
Design Programme, Indian Institute of Technology Kanpur, Kanpur, India

S. Bhattacharya et al. (eds.), *Environmental, Chemical and Medical Sensors*, Energy, Environment, and Sustainability, https://doi.org/10.1007/978-981-10-7751-7_8

1 Introduction

Nanotechnology can be defined as the design, characterization, and fabrication of engineered nanostructures or nanodevices with at least one dimension less than 100 nm (Biswas et al. 2012; Abu-Salah et al. 2010; Wang et al. 2016). A reduction in the overall size of a structure to the nanometer scale results in a substantial change in its properties, e.g., chemical, physical, thermal, mechanical, which may differ entirely from their macroscale equivalents. These nanoparticles possess a high surface-to-volume ratio providing higher binding site density for the adsorption of various biomolecules (Arruebo et al. 2009). Nanoparticles conjugated with antibodies or other biological moieties (e.g., low molecular weight ligands, peptides, proteins, DNA, plasmids) provide highly specific and selective recognition characteristics. One of the distinguished features of nanoparticles is the variation of their physical or chemical properties dependent on their size and shape. For example, by varying the size of metal nanoparticles their radiation and excitation wavelength can be tuned. This unique characteristic can be attributed to an optical phenomenon known as localized surface plasmon resonance (LSPR). LSPR occurs due to the interaction of the incident light with the surface electrons present in the conduction band (Petryayeva and Krull 2011). The phenomenon is generated by entrapped light waves in the conductive metal nanoparticles. Hence, nanoparticles offer specific physical and chemical properties that enable their utilization in a variety of domains like biomedical, energy and environment, manufacturing.

In general, there are three broad classifications of nanomaterials that are, natural, incidental and engineered (Hu et al. 2010). Natural nanomaterials are formed through natural processes and are governed by natural laws. Incidental nanomaterials are the by-products of industries (e.g., coal dust, particulates). Engineered nanomaterials are complex in shape and require specific processes for their fabrication. Based on the number of dimensions of the features, these nanomaterials can be classified into four types: 0-D, 1-D, 2-D, and 3-D (Chopra et al. 2007; Ciesielski et al. 2010; Pashchanka et al. 2010; Song et al. 2010). Zero-dimensional nanostructured materials have nanoscale dimensions in all directions, e.g., nanoparticles, nanospheres, quantum dots. One-dimensional nanostructures have non-nanoscale dimensions in a single direction such as nanorods, nanotubes, nanowires, nanobelts, nanoribbons, nanostars (Kumar et al. 2017). Two-dimensional nanostructures possess two dimensions having non-nanometric size range, e.g., graphene nanosheets, nanoplates, nanobelts, nanodiscs. Three-dimensional nanostructures contain non-nanoscale features in any three dimensions, e.g., nanotetrapods, nanoflowers, nanocombs.

This chapter presents a brief review of the bottom-up fabrication techniques used for fabrication of different shaped nanostructures and nanocomposites. It also covers the recent advancements in fabrication of ZnO-based nanostructures, DNA-based nanostructures, polymer-based nanostructures, and metal-based nanostructures and their widespread applications in the field of diagnostics, therapeutics, and others.

2 Fabrication Techniques

Nanostructures, nanomaterials, and nanocomposites can be fabricated using two different techniques, top-down and bottom-up (Bellah et al. 2012). The top-down approach involves lateral patterning of bulk materials by either subtractive or additive methods to realize nano-sized structures. Several methods are used to fabricate nanostructures using the top-down approach such as photolithography, scanning lithography, laser machining, soft lithography, nanocontact printing, nanosphere lithography, colloidal lithography, scanning probe lithography, ion implantation, diffusion, deposition. (Chi 2010; Kumar et al. 2013a). Although the top-down approach has been playing a vital role in the fabrication of nanostructures, it has several limitations such as development of imperfections in processed materials, high cost (lithographic processes), requirement of high surface finished materials, longer etching times. (Mijatovic et al. 2005; Biswas et al. 2012). In the bottom-up approach, nanostructures are fabricated by building upon single atoms or molecules. In this method, controlled segregation of atoms or molecules occurs as they are assembled into desired nanostructures (2–10 nm size range). In general, there are two basic methods utilizing the bottom-up approach, i.e., gas-phase synthesis and liquid-phase formation. Some of the methods used in bottom-up approach include plasma arcing, chemical vapor deposition process, metal organic decomposition, laser pyrolysis, molecular beam epitaxy, solgel method, wet synthesis, and self-assembly processes.

2.1 Plasma Arcing

Plasma is one of the fundamental states of matter comprising of electrons and molecules in ionic states. It maintains a condition of overall neutrality, although there may be a net positive or negative charge on certain particles. Plasma arcing method requires an ionized state of gas atoms, for which high energy is necessary to peel off the electron from its valence shell to obtain a positively charged atom. An electrical arrangement consisting of an anode and cathode is developed providing sufficient amount of electric field to transform the atoms into ions. Electrodes used are usually made up of conducting materials or mixtures of conducting and non-conducting materials. Generation of contracted plasma uses inert gas as a heat source. Emission of electrons takes place from one electrode due to the presence of high potential difference causing an electrical breakdown. A sudden avalanche of electrons results in the formation of an arc in the zone between the electrodes. Positively charged ions travel at a high velocity and are driven by the applied bias voltage toward the cathode and get deposited as nanoparticles. It is ensured that the depth of deposition consists of a few layers of atoms with each particle of the order of more than 1 nm and all particles so formed are mutually separated. The average temperature of the arc in cold plasmas is generally higher than 104 K.

2.2 Chemical Vapor Deposition (CVD)

Chemical vapor deposition process is mostly used in the semiconductor industry for depositing thin films of various materials. The process involves exposure of the substrate to one or more volatile precursors. These precursors decompose the substrate and react with it to produce the desired deposit. In the process, vaporized precursors are first adsorbed onto a substrate at a high temperature, which then react with one another or decompose and produce crystals. There are three main steps involved in the process: (i) Reactants are transported onto the growth surface by a boundary layer, (ii) chemical reactions take place on the growth surface, and (iii) by-products formed by the gas-phase reaction are removed from the growth surface. Homogeneous nucleation takes place in gas phase, whereas heterogeneous nucleation takes place in the substrate.

2.3 Molecular Beam Epitaxy (MBE)

Molecular beam epitaxy is a physical evaporation process with no chemical reactions involved. The basic difference between MBE and other epitaxy systems is that the former does not involve any chemical reactions and is instead a simple physical evaporation process. This method works on the principle of vacuum evaporation where thermal molecular and atomic beams are directly impinged on a heated substrate under ultra-high vacuum conditions (Cho and Arthur 1975). The first major advantage of the MBE process is it being a comparatively low-temperature process as compared to vapor phase epitaxy. The low-temperature characteristic of this process enables it to reduce autodoping. The second advantage of MBE is that one can have precise control over the doping process. One can achieve a growth rate as low as 0.01 μm per minute up to a maximum of 0.3 μm per minute, allowing for ultra-precise control of layer growth. With the advent of VLSI technology, it is critical to reduce all dimensions to atomic levels and thus the thickness of the epitaxial layer may also reduce further in future.

2.4 Solgel Synthesis

In the solgel process, dispersed solid nanoparticles (sols with diameter of 1–100 nm) are mixed in a homogeneous liquid medium and agglomerated to form a continuous three-dimensional network (gel) with pore diameter in the sub-micrometer domain in the liquid phase (Hench and West 1990). A sol is a liquid in which solid colloidal particles are dispersed, e.g., black inkjet ink (carbon black is dispersed in water), while a gel is a wet solid-like rigid network of interconnected nanostructures in a continuous liquid phase. Generally, there are three

approaches that have been employed to fabricate solgel film: (i) gelation of a solution of solid colloidal particles, (ii) hydrolysis and polycondensation of alkoxides followed by hypercritical drying of gels, and (iii) hydrolysis and polycondensation of alkoxide followed by aging and drying under ambient conditions. Several steps are involved in the process like mixing (formation of suspended colloidal solution by mixing of nanoparticles in water), casting of sol, gelation (formation of three-dimensional network), aging (for increasing the life of cast objects immersed in liquid), drying (removal of liquid from the interconnected continuous pore network), dehydration or chemical stabilization (to improve stability), and densification (heating the solgel at higher temperatures to eliminate pores and enhance the density, e.g., densification of alkoxide gels carried out at a temperature of 1000 °C) (Hench and West 1990). The properties of solgels depend on important parameters such as pH, type of solvent, temperature, time, catalysts and agitation mechanisms.

2.5 Molecular Self-Assembly

In general, four strategies are used for chemical synthesis of nanoparticles, i.e., sequential chemical synthesis, covalent polymerization, self-organizing synthesis, and molecular self-assembly. Molecular self-assembly (MSA) process is an ensemble of the properties of each of the above methods. MSA is a process in which atoms or molecules assemble together in equilibrium conditions to form a stable and well-defined nanophase by non-covalent bonds (Whitesides et al. 1991). All natural materials (organic or inorganic) are processed through a self-assembly route; e.g., in a natural biological process, a DNA double helix is formed through self-assembly. This approach can be used as a basic structuring mechanism to fabricate complex nanostructures (Mijatovic et al. 2005). The molecular self-assembly process is highly capable of fabricating nanostructures in the range of 1–100 nm. In order to create complex nanostructures using self-assembly process, critical parameters such as, the well-defined geometry and the specific interactions between the basic units requisite significant consideration (Rothemund 2005).

2.6 DNA Nanotechnology

Deoxyribonucleic acid (DNA) nanotechnology is the method to fabricate artificial nucleic acid nanostructures which can be utilized as nanofilters, biological scaffolds, fast performing nanowire devices, etc. Owing to its excellent physical and chemical properties, DNA has become the most widely used material for construction of nanostructures. Using nucleotide sequence-directed hybridization, DNA is able to produce duplexes and other secondary structures (Feldkamp and Niemeyer 2006). This property allows DNA molecules to self-assemble and

formulate nanoscale structures which can be employed in scaffolds, nanostructures, and nanodevices. DNA nanotechnology also utilizes the self-recognition properties of a DNA molecule to fabricate nanostructures in a desirable manner. A novel approach known as 'the DNA origami method' has been developed to fabricate two-dimensional DNA nanostructures of arbitrary shapes (Rothemund 2005).

3 Design and Synthesis of Nanostructures

3.1 ZnO-Based Nanostructures

In the recent years, various metal and metal oxide nanoparticles (MONPs) have been synthesized. Among these nanomaterials, the synthesis of metal oxides, especially zinc oxide, tin oxide, titanium dioxide nanostructures has been very prominent. The zinc oxide system in particular has shown many diverse applications owing to its relatively high and customizable band gap. Zinc oxide has been exploited for various applications like sensors (gas, bio, chemical, visible light, and ultraviolet), cosmetics, optical devices, optoelectronic devices, electrical devices, photochemical applications, solar cells, light-emitting displays, optical storages, drug delivery systems. (Gupta et al. 2013, 2014b, 2015a, b; Kumar et al. 2013b; Yao et al. 2002; Vaseem et al. 2010; Tian et al. 2003). ZnO is a semiconductor with a wide band energy gap of 3.37 eV at room temperature and a binding energy of 60 meV (Djurišić et al. 2012; Kumar et al. 2013b). The crystalline structure of ZnO is wurtzite containing hexagonal unit cells. ZnO nanostructures provide large surface area, high aspect ratio, high catalytic activity, and higher number of adsorption sites on their surfaces (Chen and Tang 2007). Also, a numerous variety of electronic and optical properties can be obtained using different ZnO nanostructures because of their rich defect chemistry (Djurišić et al. 2012).

Several fabrication techniques have been described in the literature for fabrication of ZnO nanostructures, such as sputtering, laser ablation, molecular beam epitaxy, physical vapor deposition, thermal evaporation, electrochemical deposition, template-based synthesis, and solgel methods (Yao et al. 2002; Wu et al. 2005; Chiou et al. 2003; Sun et al. 2004; Huang et al. 2001; Heo et al. 2002; Zhang et al. 2009). A variety of ZnO nanostructures such as nanoparticles (Kumar et al. 2013b), nanowires (Baruah et al. 2016; Vayssieres 2003), nanoseeds (Gupta et al. 2014b), nanorods (Vayssieres 2003), nanocombs (Huang et al. 2006), nanobelts (Fig. 1) (Sun et al. 2008), nanotubes (Sun et al. 2005), tetrapods (Qiu and Yang 2007), ribbons (Fan et al. 2009), nanopropellers (Fig. 2) (Gao and Wang 2004) have been fabricated using some of the above-mentioned fabrication technologies. ZnO quantum dots have also been fabricated for applications in bacteria diagnosis (Chen et al. 2015) and electrochemical cells (Daumann et al. 2017). Scanning electron microscopy images of a few of the above morphologies of ZnO nanostructures are shown in Fig. 3.

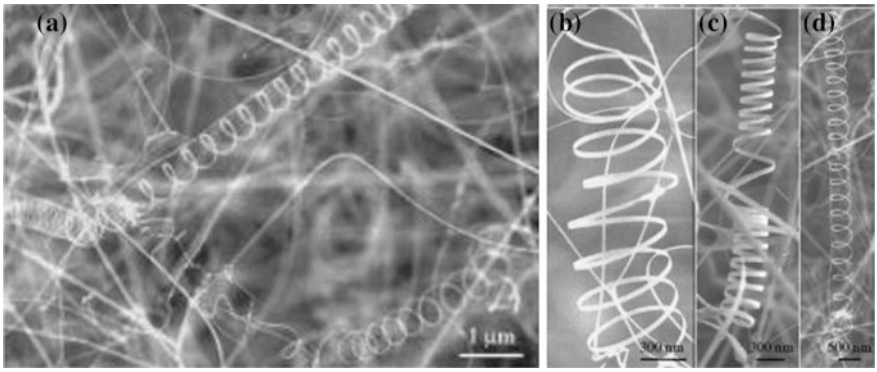

Fig. 1 a–d Image of ZnO helical nanobelts as shown in scanning electron microscope. Reproduced from Kong and Wang (2003), with permission from American Chemical Society

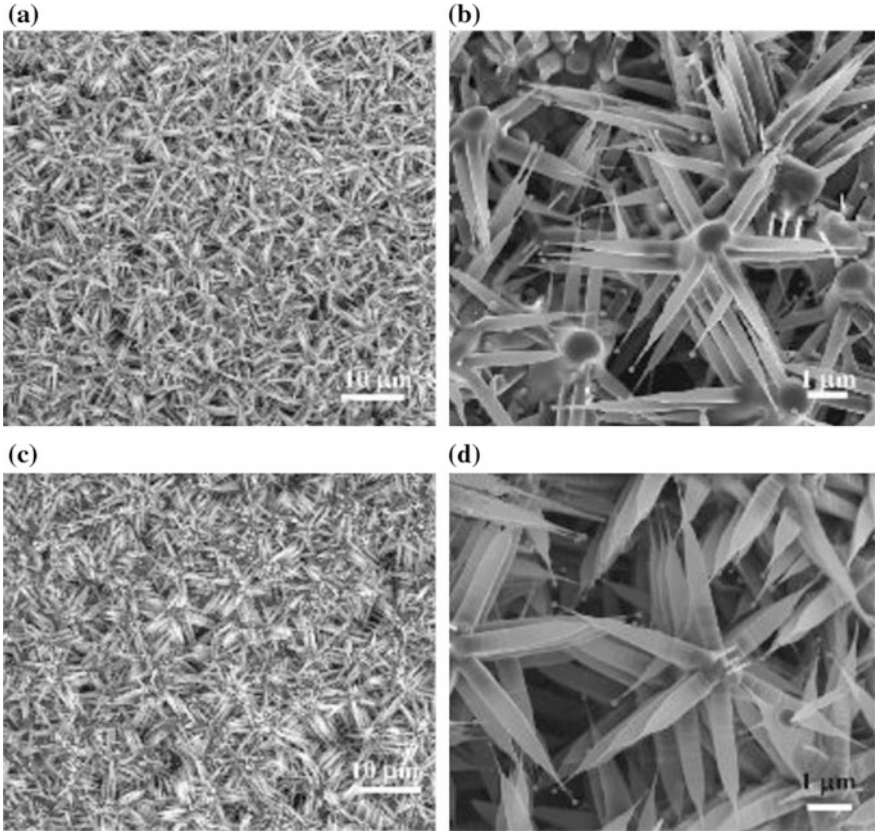

Fig. 2 a–d ZnO nanopropeller arrays as seen through a scanning electron microscope. Reproduced from Gao and Wang (2004), with permission from AIP Publishing LLC

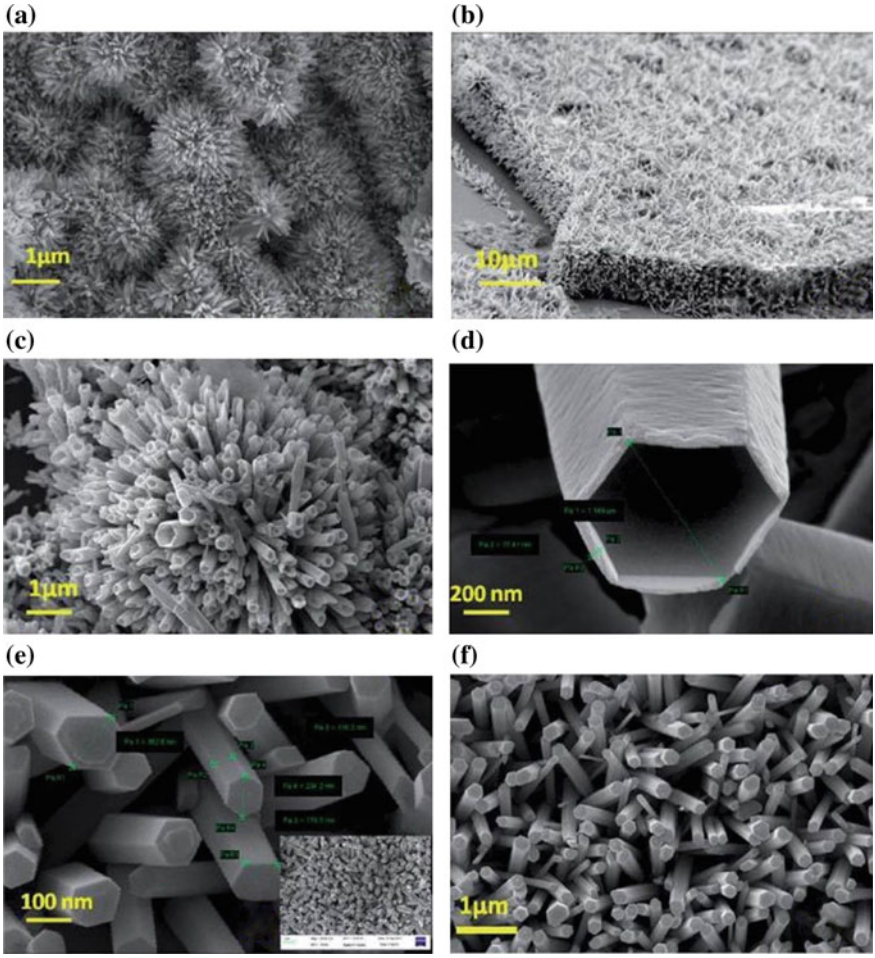

Fig. 3 FESEM images of various ZnO nanostructures morphologies at different concentrations of $Zn(NO_3)_2$. Reproduced from Gupta et al. (2014b), with permission from Royal Society of Chemistry

3.2 Polymer-Based Nanostructures

Polymers are the most extensively used biomaterials in the medical field for applications in implantation, medical devices, medical coatings, tissue engineering, and prostheses, owing to their biocompatibility with human tissues and cells (Jagur-Grodzinski 2003). Polymers are generally categorized as natural or synthetic (Broz 2010). Natural polymers extracted from the Mother Nature are biodegradable and offer excellent biocompatibility. Silk, wool, proteins (Dutta et al. 2004) (e.g., collagen, gelatin), cellulose, and DNA are some examples of naturally occurring

polymers. Due to their complex structures, modification of natural polymers is challenging. While synthetic polymers are fabricated using petroleum oils as the main constituent, there are mainly four types of synthetic polymers which include thermoplastics, thermosets, elastomers, and synthetic fibers (Peacock 2000). Examples of synthetic polymers include polydimethylsiloxane (PDMS), nylon, polypropylene, polyvinyl chloride, polystyrene, Teflon.

The fabrication methods of polymer nanostructures can be divided into two groups, template-based synthesis and template-free synthesis. Template-based synthesis includes conventional hard-template method (Parthasarathy and Martin 1994; Martin 1995; Yin and Zheng 2012), soft-template method (Meng et al. 2007), and novel wire-template method (e.g., water soluble templates, reactive self-degraded wire templates, seeding wire templates, biological wire templates) (Liang et al. 2010). On the other hand, template-free synthesis includes self-assembly method (Wan 2008), electrospinning (Li and Xia 2004), and nanoscale patterning. Template-based synthesis employs nanostructured matters as templates, over which one-dimensional polymer nanostructures can be grown. In a conventional hard-template method, micro-/nanoporous membrane materials, e.g., anodic aluminum oxide and particle track-etched membranes, are used as templates. The growth of polymer nanostructures takes place due to an electrochemical reaction of the loaded monomer solutions within the pores of these templates (Martin 1996). Reaction rate, reaction time, and temperature are vital parameters for controlling the growth of these nanostructures using conventional hard-template methods. In soft-template methods, soft amphiphilic materials like liquid crystals, surfactants, copolymers are utilized as templates. The formation of polymer nanostructures takes place as a result of the aggregation of self-assembled amphiphilic molecules through hydrogen bonding, hydrophilic–hydrophobic interactions and Van der Waals forces (Han and Foulger 2006). Novel wire-template methods are superior compared to hard-template and soft-template methods because they possess combined properties of both the above methods (Liang et al. 2010). The fabricated polymer nanostructures by this process possess high stability. In this process, preexisting one-dimensional nanomaterials are used as templates over which 1D polymer nanocomposites are grown. Template-free methods do not require any templates. Self-assembly is extensively used as a template-free chemical method for fabrication of nanostructures. Polymer nanostructures form by aggregation of nanoparticles through non-covalent bonding such as dipole–dipole interaction, electrostatic interaction, Van der Waals forces, ion–dipole interactions, and π-π stacking. Electrospinning is also a template-free physical method, in which a very high electric field is applied between the syringe containing the polymeric fluid and a conductive collector screen. A liquid jet forms when the applied electric field surpasses the surface tension of the polymeric fluid and accelerates toward the counter electrode. During this movement, the liquids get solidified and accumulate as nanofibers over the collector. Several researchers have reported the fabrication of various polymer nanostructure morphologies. Epoxy-based SU-8 polymer nanostructures with tunable high aspect ratios have been fabricated using electron beam

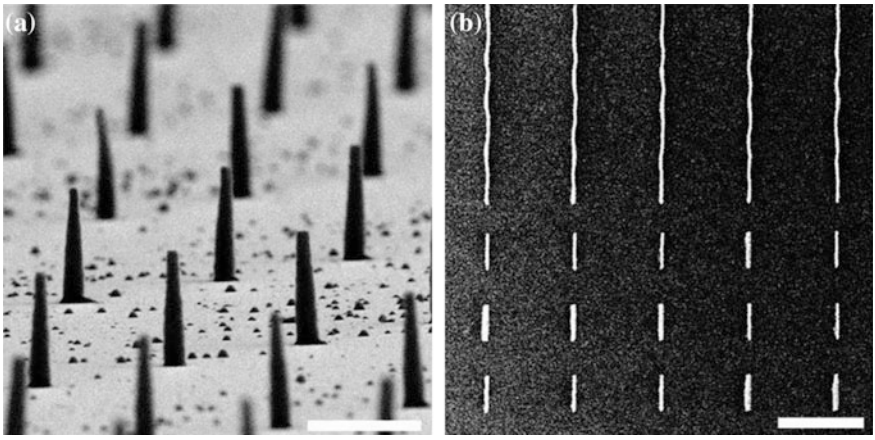

Fig. 4 SEM images of **a** nanopillars and **b** nanolines. Reproduced from Beckwith et al. (2015), with permission from the Royal Society of Chemistry

lithography (Beckwith et al. 2015). These nanostructures were synthesized on glass cover slips. Uniform arrays of SU-8 nanopillars and nanolines are shown in Fig. 4.

Ferroelectric polymer nanostructures have also been synthesized using flexible polyethylene terephthalate substrates (Song et al. 2015). A low-pressure reverse nanoimprint lithography technique has been developed that uses soft polycarbonate molds derived from recordable DVDs to fabricate nanostructures. These nanostructures are highly stable and exhibit switchable piezoelectric response and good crystallinity.

3.3 Metal-Based Nanostructures

Recently, many research fields have focused on the development of metallic nanostructures with complex shapes and various compositions in order to exploit their distinctive qualities (Gentile et al. 2016; Xia et al. 2009). Due to the high surface-to-volume ratios, metal-based nanostructured materials have been used in various domains such as catalysis, sensing, fuel cells, mechanical actuators, electrodes, point-of-care diagnostics, medicine. (Gentile et al. 2016; Jiang et al. 2012).

Various metallic nanostructures have been reported such as porous nanowires (Kolmakov et al. 2008), porous nanotubes (Lévy-Clément et al. 2009), porous nanosheets (Liang et al. 2004; Zhang et al. 2007), quantum dots (Abeyasinghe et al. 2016; Lian et al. 2015), hollow and porous nanospheres (Zhang et al. 2006). Figures 5 and 6 show SEM and TEM images of some nanowires and nanospheres.

Monodispersed bismuth particles have been fabricated by thermally decomposing bismuth acetate in boiling ethylene glycol (Wang and Xia 2004). The size of the nanospheres was varied by varying the concentration of the bismuth precursor

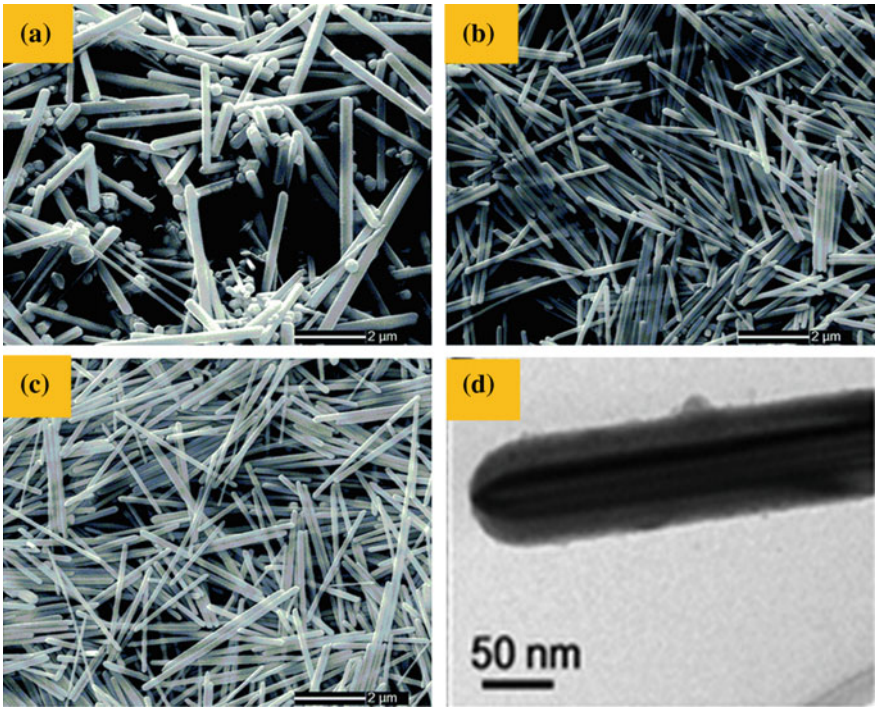

Fig. 5 **a** SEM images of silver nanowires synthesized with different amounts of $FeCl_3$: **a** 0.05 mM, **b** 0.10 mM, and **c** 0.15 mM. Adapted from Ma and Zhan (2014), with permission from the Royal Society of Chemistry. **d** TEM image of a typical silver nanowire. Reproduced from Hu et al. (2012), with permission from the Royal Society of Chemistry

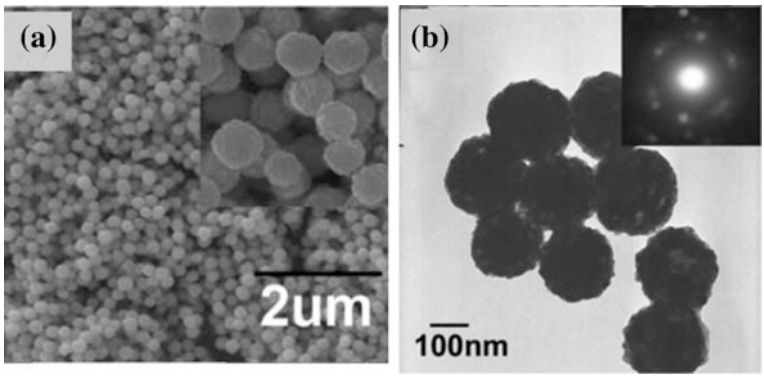

Fig. 6 **a** SEM image of CuO nanospheres. The inset shows the image at a higher resolution, **b** transmission electronic microscope image of the CuO nanospheres with an inset depicting the ED pattern of one nanosphere. Reproduced from Zhang et al. (2006), with permission from American Chemical Society

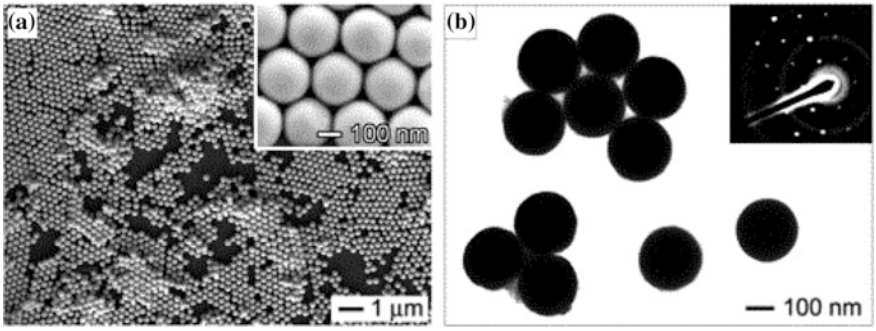

Fig. 7 **a** SEM image of bismuth nanospheres. Inset: higher resolution image, **b** TEM image of the bismuth nanospheres. Inset: SAED pattern of one nanosphere. Reproduced from Wang and Xia (2004), with permission from American Chemical Society

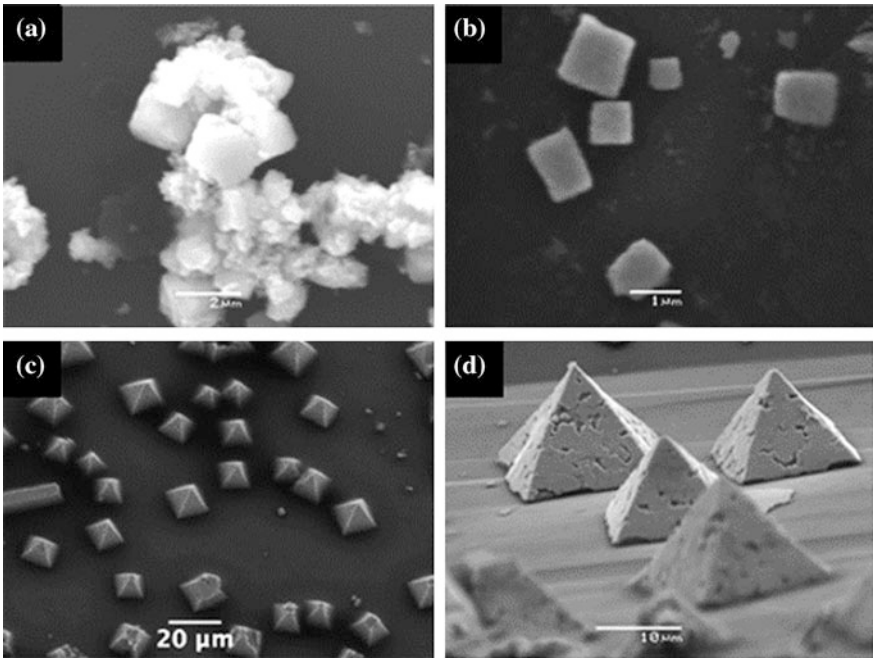

Fig. 8 **a**, **b** SEM image of cubic-shaped superlattices obtained from platinum nanocubes, **c**, **d** SEM images of pyramidal-shaped superlattices obtained from truncated nanocubes. Reproduced from Demortiere et al. (2008), with permission from American Chemical Society

and the stirring rate. The respective SEM and TEM images of the nanospheres are shown in Fig. 7.

Platinum nanocrystals have been synthesized using a liquid–liquid-phase transfer method (Demortiere et al. 2008). By controlling the nucleation and

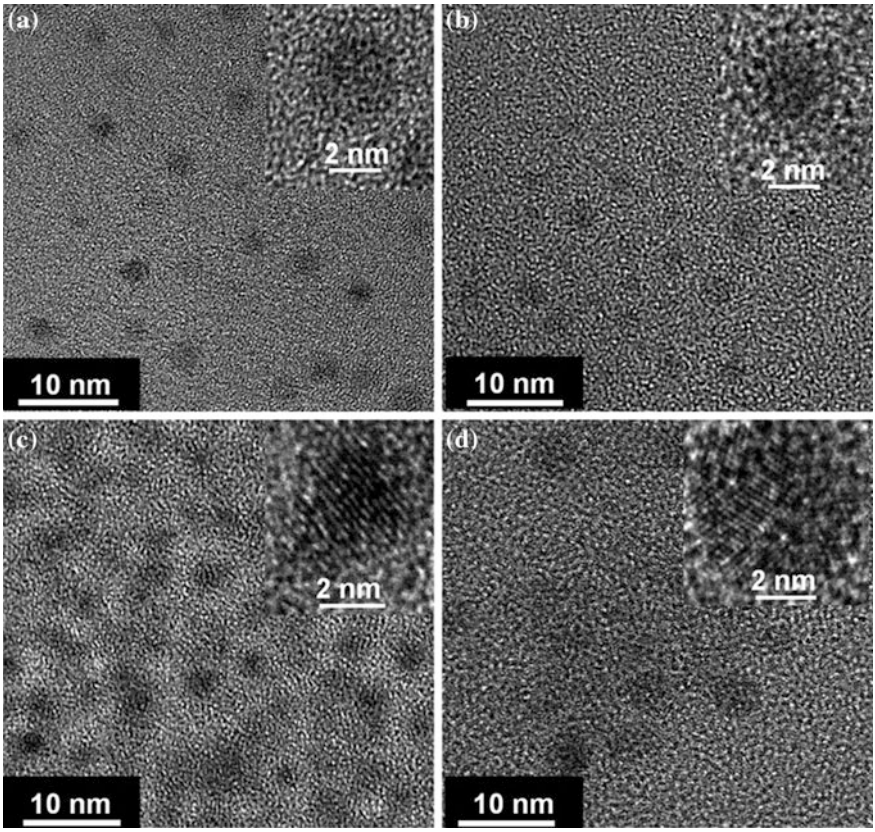

Fig. 9 HRTEM images of carbon dots using different precursors: **a** TMB, **b** DAB, **c** PY, and **d** PHA. Insets show the magnified HRTEM images. Reproduced from Yang et al. (2013), with permission from the Royal Society of Chemistry

growth process parameters, cubic and pyramidal morphologies have been achieved (Fig. 8). Further, the nanocrystals self-assemble to develop 2D and 3D supracrystals.

A soft–hard-template method has been employed for fabrication of monodispersed carbon dots (Yang et al. 2013). In order to obtain different sizes, compositions, and crystallinity, four different precursors have been used that include pyrene (PY), 1,3,5-trimethylbenzene (TMB), phenanthroline (PHA), and diaminebenzene (DAB). The TEM images of the as-synthesized carbon dots have been shown in Fig. 9.

3.4 DNA-Based Nanostructures

Deoxyribonucleic acid (DNA) is a genetic molecule in which hereditary information is encoded. It has an antiparallel double-stranded helical structure which enables its use in fabrication of nanostructures and nanodevices through a self-assembly process (Seeman 2010; Sun and Kiang 2005; Yan et al. 2003). The diameter of each strand of DNA is about 2 nm, and the helical pitch is about 3.5 nm. DNA is composed of a nitrogen-containing nucleobase (adenine, cytosine, guanine, and thymine), a sugar molecule, and a phosphate group. It has several specific characteristics that make it a preferable choice for fabrication of engineered biological nanostructures. First, DNA molecules segregate by self-assembly process so that complex structures can be fabricated with a nanometer resolution (Yan et al. 2003). Second, since the genetic information is encoded by chemical coding process, the intermolecular interaction of molecules can be easily programmed (Sun and Kiang 2005). Third, although double-stranded DNA (dsDNA) is a flexible polymer, it acts as a rigid polymer below the 50 nm size (Feldkamp and Niemeyer 2006). Therefore, the nanostructures (<50 nm) made from dsDNA can be used as rigid nanomaterials. Fourth, single-stranded DNA (ssDNA) is very flexible in comparison with dsDNA. It can be twisted to about 180° and is even capable of forming tight loops in the nanometer size. By combining the properties of dsDNA and ssDNA, complex artificial DNA nanocomposites can be fabricated. The rigidity and flexibility of these tailored nanomaterials can be controlled easily. Fifth, DNA has superior physicochemical stability as compared to proteins. The nanostructures fabricated by DNA exhibit features such as robustness and can be easily processed and synthesized.

Due to their excellent properties, DNA molecules have been used in many applications such as functional DNA nanostructures (suprastructure materials), porous, hexagonal, and 2D DNA arrays (Yan et al. 2003), DNA nanomechanical machines (Bath and Turberfield 2007; Venkataraman et al. 2007; Modi et al. 2009), and molecular computing systems (Benenson 2011; Elbaz et al. 2010; Ran et al. 2009). The fabrication of these nanostructures includes three main steps: hybridization, stably branched DNA, and synthesis of designed sequences. DNA molecules have been used to fabricate λ-DNA duplex, helix ribbon, helix tube, and DNA lattice (Fig. 10) (Lee et al. 2014). A 4 × 4 lattice has been developed by four four-armed DNA-branched junctions. Due to the large cavity size, these lattices can serve as binding sites for other molecules. For self-assembly of protein arrays, developed nanogrids were used to template streptavidin. The atomic force micrograph (AFM) of the self-assembled protein array is shown in Fig. 11. Also, a highly conductive metallic nanoelectrode has been developed by depositing silver nanomaterials on bacteriophage l DNA templates.

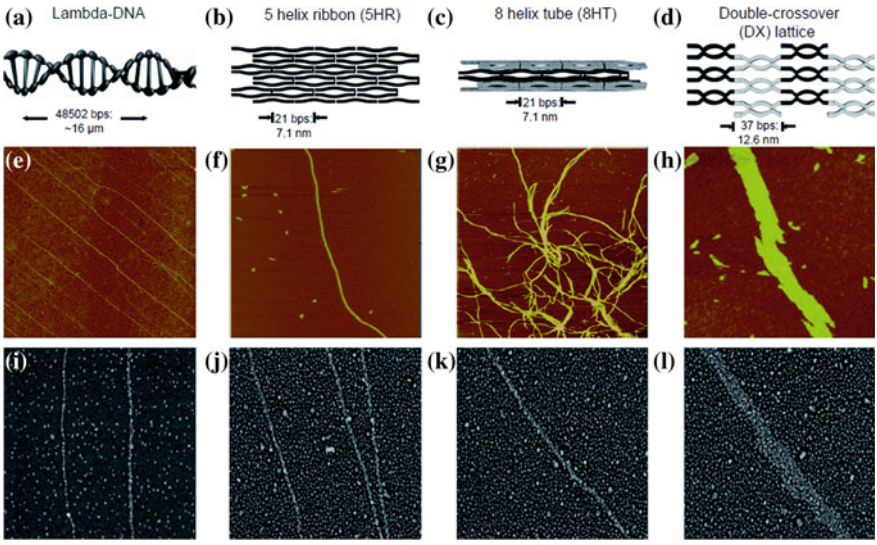

Fig. 10 **a** QD-aligned DNA nanostructures. **a–d** Schematic diagrams of the various DNA templates: **a** a λ-DNA duplex, **b** a five-helix ribbon, **c** an eight-helix tube, and **d** a double crossover (DX) DNA lattice. **e–h** AFM images of the DNA templates. AFM images in the same column as the schematic diagrams of the DNA nanostructures **a–d** correspond to those structures. **i–l** SEM images of Qdots aligned on corresponding DNA templates. Reproduced from Lee et al. (2014), with permission from the Royal Society of Chemistry

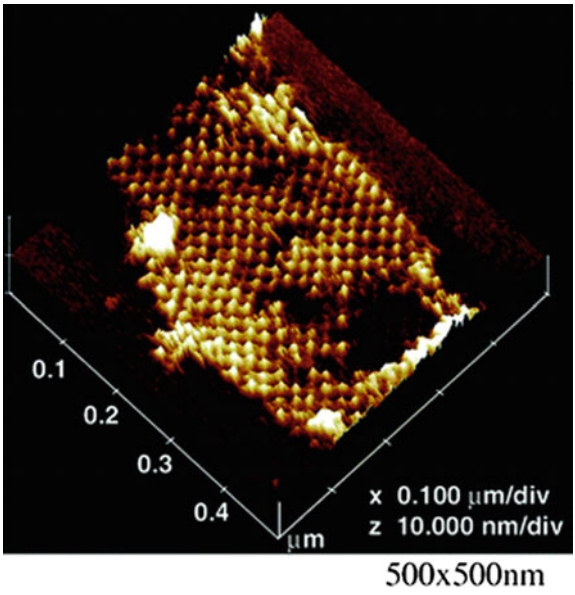

Fig. 11 Self-assembly of streptavidin array at 500 × 500 nm scale as seen through AFM. Reproduced from Christman et al. (2006), with permission from the Royal Society of Chemistry

4 Applications

Nanostructured materials have been used in a wide range of nanotechnology fields such as nanoelectronics, optoelectronics, bioelectronics, nanochemistry, sensing, nanofluidics, point-of-care diagnostics, nanomachines, therapeutics, advanced energy storages. On account of the increasing requirements of real-time sectors such as medical and health care, the diagnostic and therapeutic applications are being developed rapidly.

4.1 Diagnostic Applications

In the recent past, researchers have focused on investigating the relevance of nanostructures for development of clinical diagnostic devices. ZnO nanostructures have been used for various biological applications attributing to their non-toxic and environment-friendly nature (Vaseem et al. 2010; Gupta et al. 2014a, 2015c). ZnO nanowires have been utilized in biosensing applications by immobilization of antibodies on its surface (Gupta et al. 2014a). Goat antisalmonella was used for the immobilization purpose. Owing to the high aspect ratio, the surface of ZnO nanowires provides larger binding sites for the antibodies. For biological applications, the nanomaterials are required to be hydrophilic in nature which can be achieved by modifying the surface of nanostructures with water soluble agents. In this regard, water soluble ZnO–Au nanocomposites have been fabricated (Wang et al. 2007). These composites fulfill two purposes: ZnO provides the fluorescence, and gold nanoparticle delivers the high affinity toward the conjugation of organic

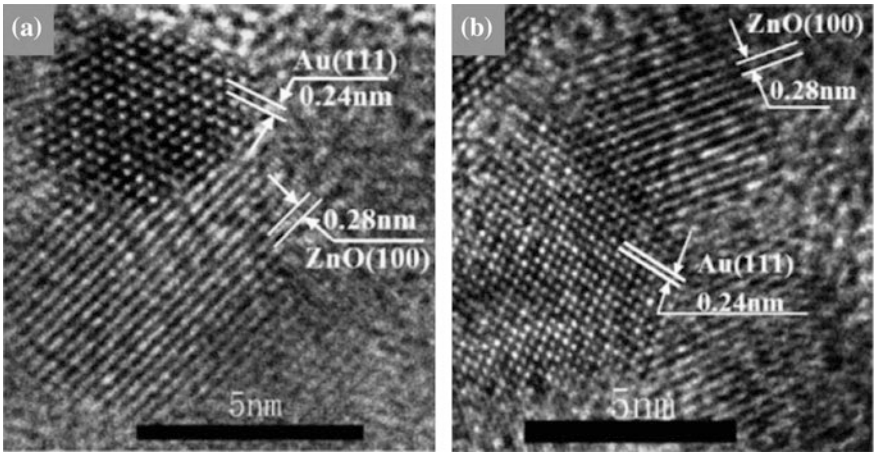

Fig. 12 **a**, **b** High-resolution TEM images of ZnO–Au nanocomposites. Reproduced from Wang et al. (2007), with permission from American Chemical Society

molecules. The transmission electron micrograph of the developed nanocomposite is shown in Fig. 12.

Several authors have reported the green synthesis of ZnO nanoparticles (Bauermann et al. 2006; Wang et al. 2007). ZnO nanoparticles have been synthesized in aqueous solution having a neutral pH (Bauermann et al. 2006). The transmission electron micrograph (TEM) and scanning electron micrograph (SEM) of these nanoparticles are shown in Fig. 13. A non-toxic buffer tris(hydroxymethyl) aminomethane acting as a polydentade ligand is used to improve the adsorption capabilities of ZnO nanoparticles.

A novel biosensor based on ZnO–Au nanocomposite has been developed for rapid and sensitive detection of microorganisms in food and water samples. Nanoporous silica film has been prepared by the traditional porogen method using poly(methylsilsesquioxane) (PMSSQ) (empirical formula: $(CH_3SiO_{1.5})_n$) as the matrix and poly(propylene glycol) (PPG) (empirical formula: $(CH(CH_3)CH_2O)n$ and molecular weight: 20,000 g/mol) as the porogen. Propylene glycol methyl ether acetate was used as a solvent for the preparation of nanoporous silica. ZnO nanostructures were grown using wet chemical synthesis, and the ZnO–Au nanocomposite was prepared by mixing the ZnO and Au nanoparticles.

Viral plant pathogens have also been detected using polypyrrole (PPy) nanoribbons (Chartuprayoon et al. 2013). Cucumber mosaic virus (CMV) has been detected by immobilizing the capture antibodies on PPy nanoribbons. The sensitivity of the device has been enhanced by reducing the thickness of PPy nanoribbons from 100 to 25 nm. The schematic representations of the biofunctionalized PPy nanoribbon and the detection of CMV are shown in Fig. 14.

Food-borne microorganisms have been detected using nucleic acid-based method (q-PCR) in a single integrated polymeric device (Nayak et al. 2013). A gold nanoparticle-assisted conjugation of IgG antibodies was employed for detection of *E. coli* bacteria. Soft lithography and replica molding techniques were used to fabricate microchannels in polydimethylsiloxane (PDMS). The fabricated microchannels are shown in Fig. 15.

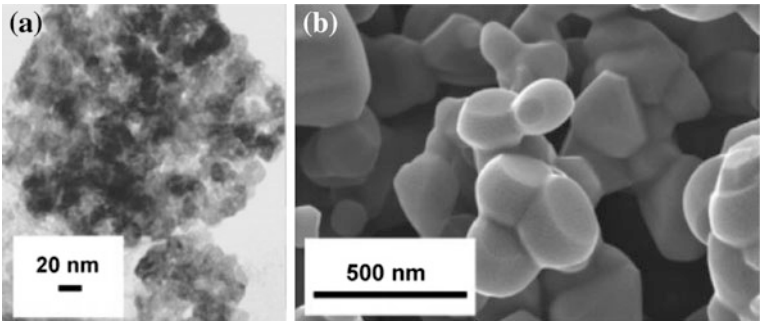

Fig. 13 **a** Transmission electron microscope images of ZnO nanoparticles. **b** SEM images of ZnO nanoparticles sintered at 1000 °C. Reproduced from Bauermann et al. (2006), with permission from American Chemical Society

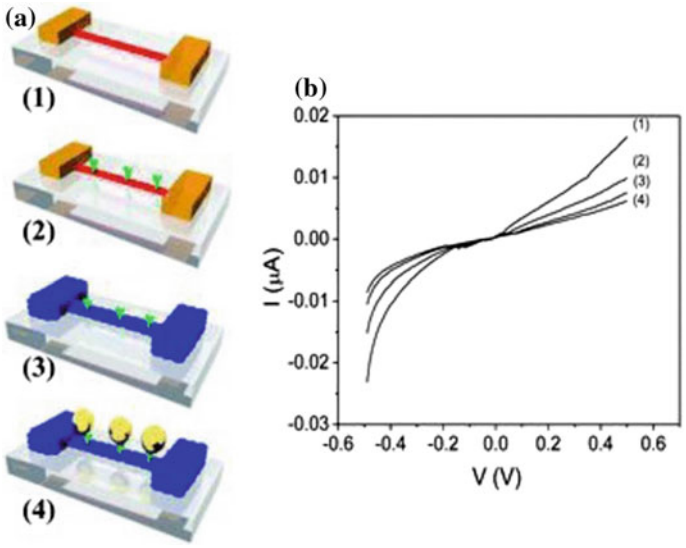

Fig. 14 **a** Schematic representations of the biofunctionalized PPy nanoribbon and the detection of CMV after each step: (1) unfunctionalized PPy nanoribbon, (2) CMV antibody functionalized PPy nanoribbon using EDC/NHS chemistry, (3) prevention of non-specific binding by immobilizing BSA onto the nanoribbon, and (4) chemiresistive detection of CMV using PPy nanoribbon and **b** corresponding I–V characteristics. Reproduced from Chartuprayoon et al. (2013), with permission from the Royal Society of Chemistry

For detection of biomarkers in human blood serum, a hybrid ZnO nanorod poly (oligo(ethylene glycol) methacrylate-*co*-glycidyl methacrylate (POEGMA-*co*-GMA) polymer brush has been reported (Hu et al. 2015). The sensitivity and specificity of an antibody microarray has been improved significantly by development of polymeric nanostructures. ZnO nanorods grown on glass slide behave as the backbone substrate over which polymer brush grows. Also, ZnO nanorods amplify the fluorescence intensity facilitating the detection of biomarkers. The POEGMA-*co*-GMA nanobrush is utilized to retain antibodies with higher densities. The limit of detection (LOD) of biomarkers in human blood serum was reported to be as low as 100 fg mL^{-1}.

In order to perform colorimetric detection of uric acid in human serum, graphene oxide-based gold nanoparticle-embedded networks have been utilized. A paper-based sensing platform has been developed that provides rapid results within 5 min and exhibits a high sensitivity of 4 ppm (Kumar et al. 2016).

Nanocantilevers have a wide range of applications in science (physical and chemical) especially in the field of sensing and point-of-care disease diagnostics. The advantages of using nanocantilevers as sensors over microsensors are that they provide higher sensitivity, are economic in terms of cost, require lower concentration of analytes (in μl), employ label-free detection, have a faster response, and consume lower power. Diagnosis of a variety of analytes for detection of various

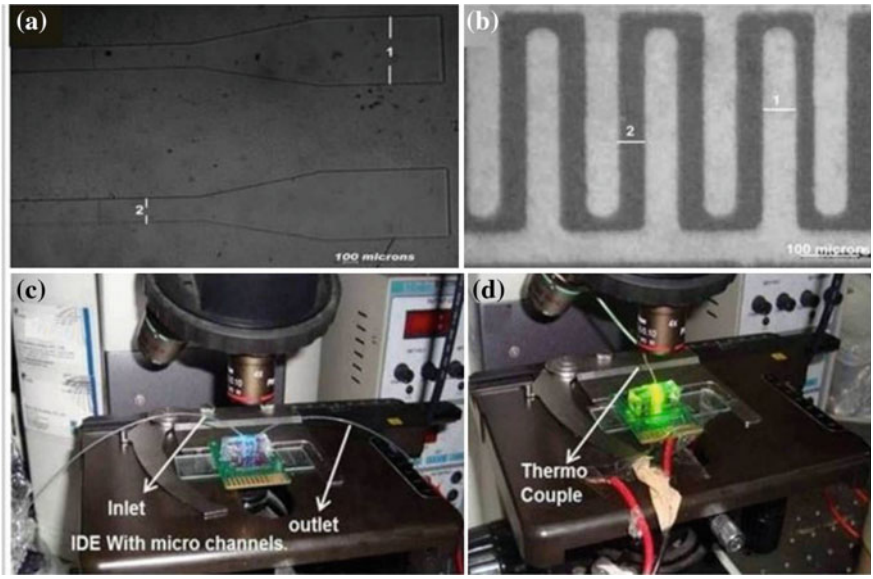

Fig. 15 Images of microchannels fabricated on polydimethylsiloxane (PDMS). **a** Image of microchannel: (1) dimension of inlet/outlet ports is around 650 µm, and (2) the main portion has a dimension of around 225 µm, **b** image of interdigitated electrodes: (1) individual width of 53.562 µm and (2) inter-electrode spacing of 42.322 µm, **c** image of dielectrophoretic capture, and **d** image of RT-PCR-based detection. Reproduced from Nayak et al. (2013), with permission from scientific reports

diseases on array of microcantilevers can be done on a single microcantilever chip leading to a higher throughput and efficiency. The surface functionalization over these cantilevers using bottom-up approaches enables sensing and detection of analytes with higher sensitivity. This methodology holds the future for high-sensitivity next-generation nanocantilever-based sensing for forthcoming point-of-care diagnostics. Single molecule detection will be the aim of researchers necessitating development of highly sensitive sensors. Gupta et al. fabricated an array of silicon nanocantilevers for detection of a single virus particle (Gupta et al. 2004). The nanocantilevers were fabricated on a p-type silicon on insulator wafer. The oxide layer was wet etched using buffered hydrofluoric acid (BHF) up to a 30 nm depth. A hybrid technique comprised of photolithography and reactive ion etching was used to pattern the cantilever beam. The etching was ceased by growing an oxide layer by means of plasma-enhanced chemical vapor deposition. BHF was used to remove the oxide layer from the side to open the windows through which silicon wafer was exposed. Finally, the cantilever beams were released through vapor phase etching using xenon difluoride. Scanning electron micrograph of the nanocantilever loaded with vaccinia virus particle is shown in Fig. 16.

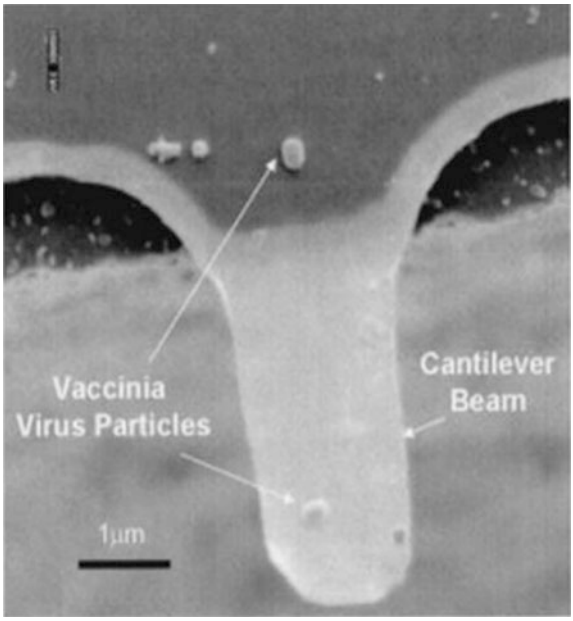

Fig. 16 SEM image of nanocantilever over which vaccinia virus particle is loaded. Reproduced from Gupta et al. (2004), with permission from AIP Publishing LLC

A nonpathogenic insect, baculovirus, has been detected using a nanoelectromechanical cantilever beam (Ilic et al. 2004). Arrays of nanomechanical free standing microcantilevers, coated with polycrystalline silicon and antibodies, were used to sense the binding of varying concentrations of baculovirus. Mechanical resonance on microcantilever-based DNA detection using gold nanoparticles has been reported (Su et al. 2003). A change in the mass of the microcantilever is induced by the DNA hybridization leading to the shift in resonance frequency of the microcantilever beam. This change is further measured. The hybridization is seen to occur through the binding of the gold nanoparticles on the microcantilever surface resulting in a chemical amplification as a result of nucleation of silver. The method reports the limit of detection of target DNA at a concentration of 0.05 nM.

DNA nanostructures have also been predominantly used for diagnostic purposes. Anisotropic, branched, and crosslinkable (ABC monomers) building blocks have been created to construct nanoarchitectures with multifunctional capabilities (Lee et al. 2009). Polymerization processes have been employed to fabricate the ABC polymeric spheres (Fig. 17). These spheres can grow only in the presence of specific target DNA molecule that leads to the detection of highly sensitive pathogens. Each ABC monomer sphere comprises of two specific quantum dots having individual ratios (1G1R). Nanoarchitectures are concocted by a combination of various quantum dots put together, with each having a unique fluorescence code. These exclusive properties enable the detection of multiple pathogens simultaneously. Three pathogens SARS, Ebola, and anthrax have been detected

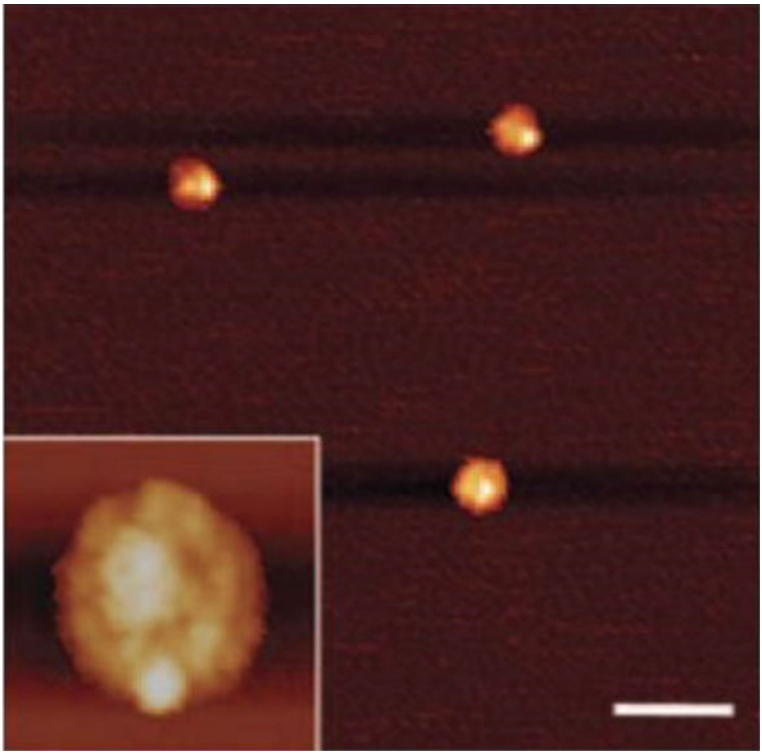

Fig. 17 AFM image of ABC polymeric spheres. A higher magnification image is shown in the inset. Scale bar, 1 μm. Reproduced from Lee et al. (2009), with permission from Macmillan Publishers Limited, part of Springer Nature

simultaneously. Distinguished relative fluorescence intensities can be visualized for detection of each pathogen (Fig. 18a–c). It has been observed that ABC polymer sphere does not construct when some unknown DNA was mixed into it (Fig. 18d).

Recently, researchers have reported the development of DNA machines (nanometer scale) that can diagnose a particular target antibody (Ranallo et al. 2015). A structural change of the DNA stems is observed when an antibody binds with the DNA nanomachines, which can also be sensed by external means or through naked eye. A light-emitting fluorophore and quencher are connected to the two single-stranded DNA stems (weak). The recognition elements capable of binding the target molecule are attached to the ends of the DNA stem. Peptides and oligonucleotides are the two most widely used recognition elements. When these elements (symbolized by the red hexagon in Fig. 19) bind to their specific target molecule, the DNA stem is broken in two parts. It separates the light-emitting fluorophore and quencher which then generate a light signal. DNA nanomachines are highly versatile and can be customized in such a way that many antibodies can

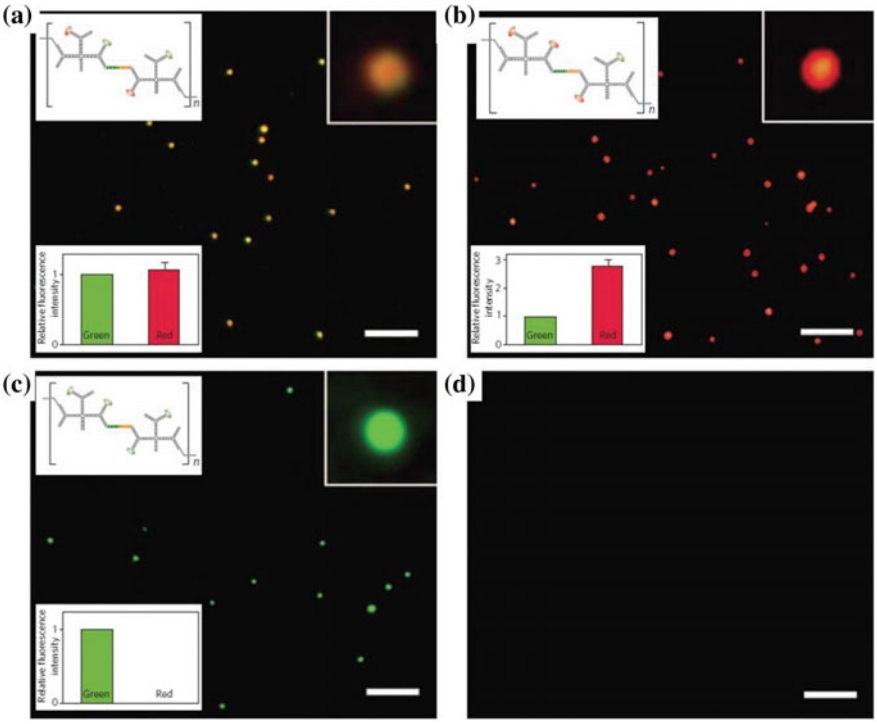

Fig. 18 **a–c** Fluorescence microscopy images of polymers with pathogen DNAs including SARS, Bacillus anthracis, and Ebola, respectively. **d** No polymerized DNA materials were observed on incubating 1G1R ABC monomers with an unrelated pathogen DNA. Scale bars, 5 μm. Reproduced from Lee et al. (2009), with permission from Macmillan Publishers Limited, part of Springer Nature

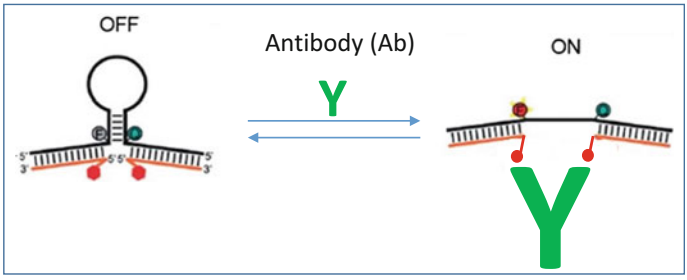

Fig. 19 Schematic diagram of antibody detection using DNA nanomachines, (F—fluorophore, and green circle denotes quencher)

be detected simultaneously with high sensitivity. Other benefits of using DNA nanomachines are that they are rapid, robust, and do not require any reagent chemicals.

Clinical diagnostic devices utilizing nanostructures have shown promise owing to their increased sensitivity, speed, portability, and inexpensive nature as compared to conventional diagnostic techniques.

4.2 Therapeutic Applications

The exponentially growing potential of nanostructures has envisaged several applications in the treatment of numerous medical ailments. ZnO nanoparticles have been used to augment the mechanical and antimicrobial properties of dental filler material (Gupta et al. 2015c). ZnO–HAP nanocomposite was fabricated by mixing ZnO nanoparticles with hydroxyapatite (HAP) using a wet chemical route through ultrasonication process. The antimicrobial properties of this nanocomposite have been investigated for *E. coli* DH5α and Streptococcus mutans, and a substantial enhancement in the antimicrobial activity has been reported. ZnO nanostructures have also been used for anticancer studies and their action against human brain tumor U87 and cervical cancer HeLa (Wahab et al. 2011). Under all effective concentrations, these nanostructures revealed reduced cytotoxicity against normal human HEK cells. ZnO nanoparticles have also shown a strong special capability to destroy cancerous T cells (Hanley et al. 2008). It has also been reported that ZnO nanostructures exhibit excellent ultraviolet blocking characteristics (Smijs and Pavel 2011; Kathirvelu et al. 2009). There are primarily three types of ultraviolet rays contained in natural sunlight, i.e., UV-A (320–400 nm), UV-B (290–320 nm), and UV-C (250–290 nm) (Vaseem et al. 2010). Among all of them, UV-A and UV-B are more dangerous as they may cause skin cancer. In order to protect the human skin from direct exposure of these rays, a ZnO–TiO_2 (titanium dioxide) nanocomposite (Smijs and Pavel 2011) has been developed in which TiO_2 blocks the UV-B rays while ZnO nanoparticles block the UV-A rays. ZnO nanoparticles have been coated on fabrics to make them UV resistant (Kathirvelu et al. 2009). Since the size of ZnO particles is in the nanometer range, it binds very well to the fabric owing to the Van der Waals force of attraction and the adhesion is retained even after multiple washings (Fig. 20).

Self-assembled amphiphilic polymer nanostructures have become efficient nanocarriers for targeted delivery of anticancer therapeutics (Wiradharma et al. 2009). Polysaccharide chitosan-based polymeric nanostructures have been employed in delivery of hydrophilic and lipophilic drugs onto the eye surfaces (de la Fuente et al. 2010). Therapeutic efficiency against pancreatic tumor has been enhanced by using a bundled assembly of helical polymeric nanostructures laden with platinum drugs (Mochida et al. 2014). Due to their structural diversity, biocompatibility, and uniformity in structures, DNA-based nanostructures have been extensively used for therapeutic applications. The growth of cancer cells has been

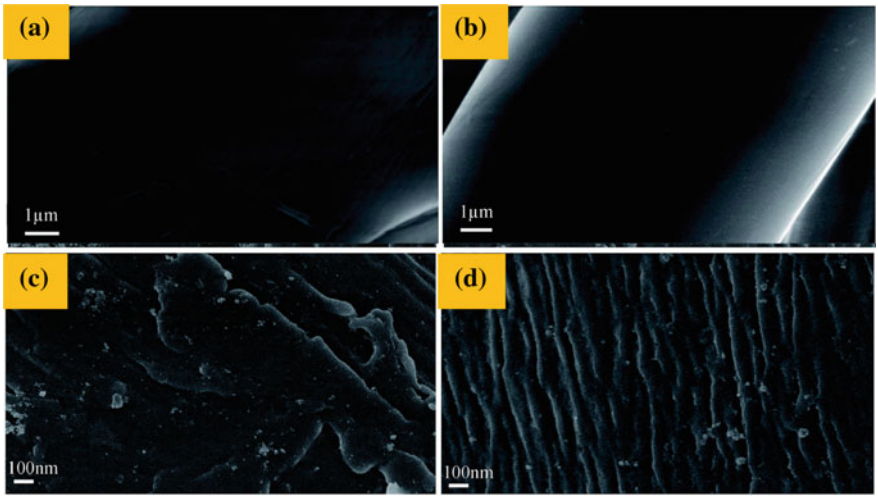

Fig. 20 FESEM images of **a**, **b** 100% cotton and **c**, **d** ZnO nanoparticles embedded fabric. Reproduced from Bușilă et al. (2015), with permission from the Royal Society of Chemistry

inhibited by combining AS1411 aptamers into DNA pyramids without using any transfection reagents (Charoenphol and Bermudez 2014).

Electroporation is a commonly used method for gene delivery, which requires high voltage ($\sim$100–500 k V/m) for DNA transfection. However, a major portion of the exposed cells are completely destroyed as a result of this high voltage. In order to overcome this problem, molecular delivery using shock wave-assisted methods has been widely employed (Lauer et al. 1997; Kodama et al. 2002). These shock waves can be generated using nanoenergetic materials, which can further be utilized for gene transfection purposes (Gangopadhyay et al. 2011; Patel et al. 2015).

The small size of the nanostructures provides the requisite potential in this domain, which is enablement of easy access to the internal parts of the body without affecting other body functions. Although they can be utilized for therapeutics, the materials that they are made of possess a potential danger to the human body. Hence, further research is required to critically analyze the biocompatibility and biodegradability of these materials.

4.3 Miscellaneous Applications

Apart from the mainstream applications of nanostructures, nanostructures have been largely explored for various other outlying areas, e.g., environmental protection, bio-imaging, water purification. For example, ZnO nanoparticles possess capabilities to remove organic dyes and hazardous materials from polluted water.

Dye-sensitized solar cells (DSSCs) utilize ZnO aggregate films as photoelectrodes (Zhang et al. 2008). Polyol-mediated precipitation of zinc acetate in diethylene glycol has been used for synthesis of ZnO aggregates. It has been found that the size of ZnO aggregates can be manipulated by controlling the concentration of zinc acetate, rate of heating, etc. The drop-cast method has been used for the fabrication of photoelectrode film by depositing the ZnO aggregates on the fluorine-doped tin oxide glass substrates. The morphologies of ZnO films at different temperatures are shown in Fig. 21.

For the fabrication of a nonvolatile memory device, conductive polymer nanostructures have been prepared from graphene oxide and poly (3,4-ethylenedioxythiophene)-poly(styrenesulfonate) (PEDOT-PSS)-based composites (Ray et al. 2015). Silver electrodes of thickness 200 nm and diameter 100 μm were deposited on the fabricated composites to examine their electrical properties. The linear voltage–current relationships of polymer nanostructures confirmed its conductive nature. Conductive polymer nanostructures can be used for harvesting energy from solar light using photocatalysis under visible light (Ghosh et al. 2015). One-dimensional nanofibers made of poly(diphenylbutadiyne) (PDPB) have been synthesized by photopolymerization using a novel soft-template approach. These nanofibers are highly efficient for degradation of pollutants under visible light. It has been observed that the nanofibers are very stable and exhibit higher photocatalytic activity than bulk PDPB. The organic pollutants such as methyl orange and phenol are highly toxic and are a threat to the ecosystem. These pollutants have been degraded by photocatalysis process. The nano-PDPB nanofibers possess good photocatalytic activity for methyl orange under visible light. A 75% degradation of methyl orange has been achieved after 240 min of irradiation. The change in morphology of PDPB nanostructures after photocatalysis is shown in Fig. 22.

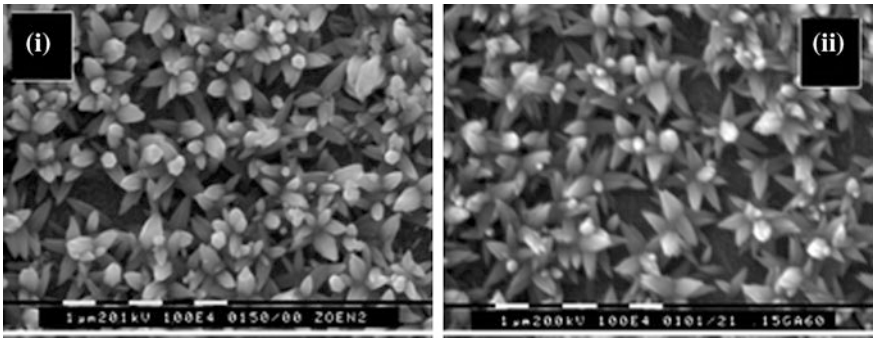

Fig. 21 Scanning electron microscopic images of developed ZnO films from en-baths (70 °C, pH 11) containing: i. zinc acetate; ii. zinc chloride. Reproduced from Govender et al. (2004), with permission from the Royal Society of Chemistry

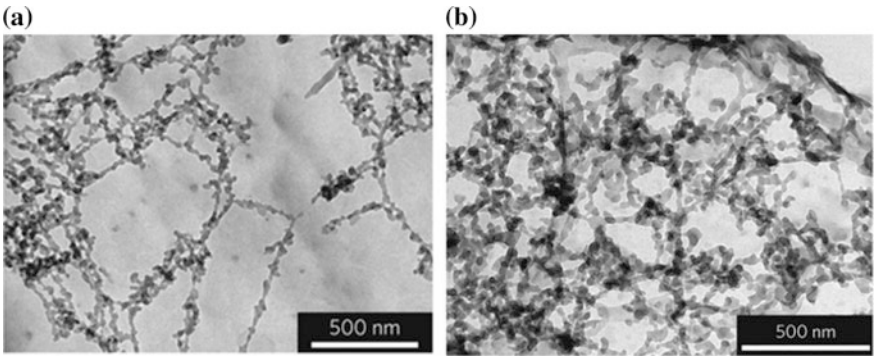

Fig. 22 **a** TEM image of fabricated PDPB nanostructures, **b** TEM image of the PDPB nanofibers after methyl orange degradation under visible light irradiation. Reproduced from Ghosh et al. (2015), with permission from Macmillan Publishers Limited, part of Springer Nature

Studies have yielded fascinating results in these domains for nanostructures made of single as well as composite nanomaterials. Such varied applications of nanostructures have enabled the advancement of the nanotechnology sector to great extents.

5 Conclusion

In this chapter, the fabrication of nanostructures by employing bottom-up approach has been described. Some basic processes used in the bottom-up approach have been discussed in detail. The latest fabrication technologies for the fabrication of ZnO nanostructures, DNA nanostructures, polymer-based nanostructures, and metal-based nanostructures have also been discussed. It is seen that these nanostructures have wide applications as, sensors (gas, bio, chemical, visible light, and ultraviolet), cosmetics, optical devices, optoelectronics, electrical devices, photo-chemistry, solar cells and light-emitting displays separation, optical storages, and drug delivery. DNA nanostructures have been utilized in drug delivery, nanoswitches, computing, etc. Owing to characteristics like high sensitivity, inexpensive, non-hazardous, and faster response to analytes, nanostructures have been employed for sensing, detection, screening of viruses, etc. It is evident that nanotechnology is an emerging field with potential to revolutionize the therapeutics and diagnostics industry. Advancements in the area of nanostructure fabrication have allowed to achieve development of highly sensitive and specific sensors. The integration of these nanostructures for therapeutic and diagnostic purposes could facilitate the engineering of improved nanostructures specific to required biomedical applications.

References

Abeyasinghe N, Kumar S, Sun K, Mansfield JF, Jin R, Goodson T III (2016) Enhanced emission from single isolated gold quantum dots investigated using two-photon-excited fluorescence near-field scanning optical microscopy. J Am Chem Soc 138(50):16299–16307

Abu-Salah KM, Ansari AA, Alrokayan SA (2010) DNA-based applications in nanobiotechnology. Biomed Res Int 2010:15

Arruebo M, Valladares M, González-Fernández Á (2009) Antibody-conjugated nanoparticles for biomedical applications. J Nanomater 2009:37

Baruah S, Thanachayanont C, Dutta J (2016) Growth of ZnO nanowires on nonwoven polyethylene fibers. Sci Technol Adv Mater 9:8

Bath J, Turberfield AJ (2007) DNA nanomachines. Nat Nanotechnol 2(5):275–284

Bauermann LP, Bill J, Aldinger F (2006) Bio-friendly synthesis of ZnO nanoparticles in aqueous solution at near-neutral pH and low temperature. J Phys Chem B 110(11):5182–5185

Beckwith KS, Cooil SP, Wells JW, Sikorski P (2015) Tunable high aspect ratio polymer nanostructures for cell interfaces. Nanoscale 7(18):8438–8450

Bellah MM, Christensen SM, Iqbal SM (2012) Nanostructures for medical diagnostics. J Nanomater 2012:2

Benenson Y (2011) Biocomputing: DNA computes a square root. Nat Nanotechnol 6(8):465–467

Biswas A, Bayer IS, Biris AS, Wang T, Dervishi E, Faupel F (2012) Advances in top–down and bottom–up surface nanofabrication: techniques, applications & future prospects. Adv Colloid Interface Sci 170(1):2–27

Broz P (2010) Contents. In: Polymer-based Nanostructures. pp P009–P015

Buşilă M, Mușat V, Textor T, Mahltig B (2015) Synthesis and characterization of antimicrobial textile finishing based on Ag: ZnO nanoparticles/chitosan biocomposites. RSC Adv 5 (28):21562–21571

Charoenphol P, Bermudez H (2014) Aptamer-targeted DNA nanostructures for therapeutic delivery. Mol Pharm 11(5):1721–1725

Chartuprayoon N, Rheem Y, Ng JC, Nam J, Chen W, Myung NV (2013) Polypyrrole nanoribbon based chemiresistive immunosensors for viral plant pathogen detection. Anal Methods 5 (14):3497–3502

Chen H, Zhang M, Li B, Chen D, Dong X, Wang Y, Gu Y (2015) Versatile antimicrobial peptide-based ZnO quantum dots for in vivo bacteria diagnosis and treatment with high specificity. Biomaterials 53:532–544

Chen J-C, Tang C-T (2007) Preparation and application of granular ZnO/Al 2 O 3 catalyst for the removal of hazardous trichloroethylene. J Hazard Mater 142(1):88–96

Chi L (2010) Nanotechnology: volume 8: nanostructured surfaces, vol 7. Wiley, Weinheim

Chiou W-T, Wu W-Y, Ting J-M (2003) Growth of single crystal ZnO nanowires using sputter deposition. Diamond Relat Mater 12(10):1841–1844

Cho A, Arthur J (1975) Molecular beam epitaxy. Prog Solid State Chem 10:157–191

Chopra N, Gavalas VG, Bachas LG, Hinds BJ, Bachas LG (2007) Functional one-dimensional nanomaterials: applications in nanoscale biosensors. Anal Lett 40(11):2067–2096

Christman KL, Enriquez-Rios VD, Maynard HD (2006) Nanopatterning proteins and peptides. Soft Matter 2(11):928–939

Ciesielski A, Palma CA, Bonini M, Samorì P (2010) Towards supramolecular engineering of functional nanomaterials: pre-programming multi-component 2D self-assembly at solid-liquid interfaces. Adv Mater 22(32):3506–3520

Daumann S, Andrzejewski D, Di Marcantonio M, Hagemann U, Wepfer S, Vollkommer F, Bacher G, Epple M, Nannen E (2017) Water-free synthesis of ZnO quantum dots for application as an electron injection layer in light-emitting electrochemical cells. J Mater Chem C 5(9):2344–2351

de la Fuente M, Raviña M, Paolicelli P, Sanchez A, Seijo B, Alonso MJ (2010) Chitosan-based nanostructures: a delivery platform for ocular therapeutics. Adv Drug Deliv Rev 62(1):100–117

Demortiere A, Launois P, Goubet N, Albouy P-A, Petit C (2008) Shape-controlled platinum nanocubes and their assembly into two-dimensional and three-dimensional superlattices. J Phys Chem B 112(46):14583–14592

Djurišić AB, Chen X, Leung YH, Ng AMC (2012) ZnO nanostructures: growth, properties and applications. J Mater Chem 22(14):6526–6535

Dutta PK, Dutta J, Tripathi V (2004) Chitin and chitosan: chemistry, properties and applications. J Sci Ind Res 63(1):20–31

Elbaz J, Lioubashevski O, Wang F, Remacle F, Levine RD, Willner I (2010) DNA computing circuits using libraries of DNAzyme subunits. Nat Nanotechnol 5(6):417–422

Fan X, Zhang ML, Shafiq I, Zhang WJ, Lee CS, Lee ST (2009) ZnS/ZnO heterojunction nanoribbons. Adv Mater 21(23):2393–2396

Feldkamp U, Niemeyer CM (2006) Rational design of DNA nanoarchitectures. Angew Chem Int Ed 45(12):1856–1876

Gangopadhyay S, Apperson S, Gangopadhyay K, Bezmelnitsyn A, Thiruvengadathan R, Kraus M, Shende R, Hossain M, Subramanian S, Bhattacharya S (2011) Shock wave and power generation using on-chip nanoenergetic material. US Patent U.S. Patent 8,066,831

Gao P, Wang ZL (2004) Nanopropeller arrays of zinc oxide. Appl Phys Lett 84:2883–2885

Gentile A, Ruffino F, Grimaldi MG (2016) Complex-morphology metal-based nanostructures: fabrication, characterization, and applications. Nanomaterials 6(6):110

Ghosh S, Kouamé NA, Ramos L, Remita S, Dazzi A, Deniset-Besseau A, Beaunier P, Goubard F, Aubert P-H, Remita H (2015) Conducting polymer nanostructures for photocatalysis under visible light. Nat Mater 14(5):505–511

Govender K, Boyle DS, Kenway PB, O'Brien P (2004) Understanding the factors that govern the deposition and morphology of thin films of ZnO from aqueous solution. J Mater Chem 14 (16):2575–2591

Gupta A, Akin D, Bashir R (2004) Single virus particle mass detection using microresonators with nanoscale thickness. Appl Phys Lett 84(11):1976–1978

Gupta A, Mondal K, Sharma A, Bhattacharya S (2015a) Superhydrophobic polymethyl-silsesquioxane pinned one dimensional ZnO nanostructures for water remediation through photo-catalysis. RSC Adv 5(57):45897–45907

Gupta A, Nayak M, Singh D, Bhattacharya S (2014a) Antibody immobilization for ZnO nanowire based biosensor application. In: MRS proceedings. Cambridge University Press, pp 33–39

Gupta A, Pandey S, Nayak M, Maity A, Majumder SB, Bhattacharya S (2014b) Hydrogen sensing based on nanoporous silica-embedded ultra dense ZnO nanobundles. RSC Adv 4(15):7476–7482

Gupta A, Pandey SS, Bhattacharya S (2013) High aspect ZnO nanostructures based hydrogen sensing. In: Proceeding of international conference on recent trends in applied physics and material science: RAM 2013, vol 1. AIP Publishing, pp 291–292

Gupta A, Saurav JR, Bhattacharya S (2015b) Solar light based degradation of organic pollutants using ZnO nanobrushes for water filtration. RSC Adv 5(87):71472–71481

Gupta A, Singh D, Raj P, Gupta H, Verma S, Bhattacharya S (2015c) Investigation of ZnO-hydroxyapatite nanocomposite incorporated in restorative glass ionomer cement to enhance its mechanical and antimicrobial properties. J Bionanosci 9(3):190–196

Han MG, Foulger SH (2006) Facile synthesis of poly (3, 4-ethylenedioxythiophene) nanofibers from an aqueous surfactant solution. Small 2(10):1164–1169

Hanley C, Layne J, Punnoose A, Reddy K, Coombs I, Coombs A, Feris K, Wingett D (2008) Preferential killing of cancer cells and activated human T cells using ZnO nanoparticles. Nanotechnology 19(29):295103

Hench LL, West JK (1990) The sol-gel process. Chem Rev 90(1):33–72

Heo Y, Varadarajan V, Kaufman M, Kim K, Norton D, Ren F, Fleming P (2002) Site-specific growth of ZnO nanorods using catalysis-driven molecular-beam epitaxy. Appl Phys Lett 81 (16):3046–3048

Hu H, Onyebueke L, Abatan A (2010) Characterizing and modeling mechanical properties of nanocomposites-review and evaluation. J Miner Mater Charact Eng 9(04):275

Hu M, Gao J, Dong Y, Yang S, Li RK (2012) Rapid controllable high-concentration synthesis and mutual attachment of silver nanowires. RSC Adv 2(5):2055–2060

Hu W, Liu Y, Chen T, Liu Y, Li CM (2015) Hybrid ZnO nanorod-polymer brush hierarchically nanostructured substrate for sensitive antibody microarrays. Adv Mater 27(1):181–185

Huang MH, Wu Y, Feick H, Tran N, Weber E, Yang P (2001) Catalytic growth of zinc oxide nanowires by vapor transport. Adv Mater 13(2):113–116

Huang Y, Zhang Y, Bai X, He J, Liu J, Zhang X (2006) Bicrystalline zinc oxide nanocombs. J Nanosci Nanotechnol 6(8):2566–2570

Ilic B, Yang Y, Craighead H (2004) Virus detection using nanoelectromechanical devices. Appl Phys Lett 85(13):2604–2606

Jagur-Grodzinski J (2003) Biomedical applications of polymers 2001–2002. e-Polymers 3(1):141–176c

Jiang J, Li Y, Liu J, Huang X, Yuan C, Lou XWD (2012) Recent advances in metal oxide-based electrode architecture design for electrochemical energy storage. Adv Mater 24(38):5166–5180

Kathirvelu S, D'souza L, Dhurai B (2009) UV protection finishing of textiles using ZnO nanoparticles. Indian J Fibre Text Res 34(3):267–273

Kodama T, Doukas AG, Hamblin MR (2002) Shock wave-mediated molecular delivery into cells. biochimica et biophysica acta (BBA)-molecular. Cell Res 1542(1):186–194

Kolmakov A, Chen X, Moskovits M (2008) Functionalizing nanowires with catalytic nanoparticles for gas sensing application. J Nanosci Nanotechnol 8(1):111–121

Kong XY, Wang ZL (2003) Spontaneous polarization-induced nanohelixes, nanosprings, and nanorings of piezoelectric nanobelts. Nano Lett 3(12):1625–1631

Kumar S, Bhushan P, Bhattacharya S (2016) Development of a paper-based analytical device for colorimetric detection of uric acid using gold nanoparticles–graphene oxide (AuNPs–GO) conjugates. Anal Methods 8(38):6965–6973. https://doi.org/10.1039/c6ay01926a

Kumar S, Bhushan P, Bhattacharya S (2017) Facile synthesis of Au@Ag–Hemin decorated reduced graphene oxide sheets: a novel peroxidase mimetic for ultrasensitive colorimetric detection of hydrogen peroxide and glucose. RSC Adv 7:37568–37577. https://doi.org/10.1039/c7ra06973a

Kumar S, Dubey AK, Pandey AK (2013a) Computer-aided genetic algorithm based multi-objective optimization of laser trepan drilling. Int J Precis Eng Manuf 14(7):1119–1125

Kumar SS, Venkateswarlu P, Rao VR, Rao GN (2013b) Synthesis, characterization and optical properties of zinc oxide nanoparticles. Int Nano Lett 3(1):1–6

Lauer U, Bürgelt E, Squire Z, Messmer K, Hofschneider P, Gregor M, Delius M (1997) Shock wave permeabilization as a new gene transfer method. Gene therapy 4(7):710–715

Lee J, Lee J, Yeon SM, Min S, Kim J, Choi H, Kim S, Koo J, Kim K, Park SH (2014) Assembling CdSe/ZnS core–shell quantum dots on localized DNA nanostructures. RSC Adv 4(95):53201–53205

Lee JB, Roh YH, Um SH, Funabashi H, Cheng W, Cha JJ, Kiatwuthinon P, Muller DA, Luo D (2009) Multifunctional nanoarchitectures from DNA-based ABC monomers. Nat Nanotechnol 4(7):430–436

Lévy-Clément C, Elias J, Tena-Zaera R (2009) ZnO/CdSe nanowires and nanotubes: formation, properties and applications. physica status solidi (c) 6(7):1596–1600

Li D, Xia Y (2004) Electrospinning of nanofibers: reinventing the wheel? Adv Mater 16 (14):1151–1170

Lian Z, Wang W, Xiao S, Li X, Cui Y, Zhang D, Li G, Li H (2015) Plasmonic silver quantum dots coupled with hierarchical TiO2 nanotube arrays photoelectrodes for efficient visible-light photoelectrocatalytic hydrogen evolution. Sci Rep 5:10461

Liang HW, Liu S, Yu SH (2010) Controlled synthesis of one-dimensional inorganic nanostructures using pre-existing one-dimensional nanostructures as templates. Adv Mater 22(35):3925–3937
Liang Z-H, Zhu Y-J, Hu X-L (2004) β-nickel hydroxide nanosheets and their thermal decomposition to nickel oxide nanosheets. J Phys Chem B 108(11):3488–3491
Ma J, Zhan M (2014) Rapid production of silver nanowires based on high concentration of $AgNO_3$ precursor and use of $FeCl_3$ as reaction promoter. RSC Adv 4(40):21060–21071
Martin CR (1995) Template synthesis of electronically conductive polymer nanostructures. Acc Chem Res 28(2):61–68
Martin CR (1996) Membrane-based synthesis of nanomaterials. Chem Mater 8(8):1739–1746
Meng L, Lu Y, Wang X, Zhang J, Duan Y, Li C (2007) Facile synthesis of straight polyaniline nanostick in hydrogel. Macromolecules 40(9):2981–2983
Mijatovic D, Eijkel J, Den Van, Berg A (2005) Technologies for nanofluidic systems: top-down versus bottom-up—a review. Lab Chip 5(5):492–500
Mochida Y, Cabral H, Miura Y, Albertini F, Fukushima S, Osada K, Nishiyama N, Kataoka K (2014) Bundled assembly of helical nanostructures in polymeric micelles loaded with platinum drugs enhancing therapeutic efficiency against pancreatic tumor. ACS Nano 8(7):6724–6738
Modi S, Swetha M, Goswami D, Gupta GD, Mayor S, Krishnan Y (2009) A DNA nanomachine that maps spatial and temporal pH changes inside living cells. Nat Nanotechnol 4(5):325–330
Nayak M, Singh D, Singh H, Kant R, Gupta A, Pandey SS, Mandal S, Ramanathan G, Bhattacharya S (2013) Integrated sorting, concentration and real time PCR based detection system for sensitive detection of microorganisms. Sci Rep 3:3266
Parthasarathy RV, Martin CR (1994) Synthesis of polymeric microcapsule arrays and their use for enzyme immobilization. Nature 369(6478):298
Pashchanka M, Hoffmann RC, Gurlo A, Schneider JJ (2010) Molecular based, chimie douce approach to 0d and 1d indium oxide nanostructures. Evaluation of their sensing properties towards co and h 2. J Mater Chem 20(38):8311–8319
Patel VK, Saurav JR, Gangopadhyay K, Gangopadhyay S, Bhattacharya S (2015) Combustion characterization and modeling of novel nanoenergetic composites of Co_3O_4/nAl. RSC Adv 5 (28):21471–21479
Peacock A (2000) Handbook of polyethylene: structures: properties, and applications. CRC Press, Boca Raton, FL
Petryayeva E, Krull UJ (2011) Localized surface plasmon resonance: nanostructures, bioassays and biosensing—a review. Anal Chim Acta 706(1):8–24
Qiu Y, Yang S (2007) ZnO nanotetrapods: controlled vapor-phase synthesis and application for humidity sensing. Adv Funct Mater 17(8):1345–1352
Ran T, Kaplan S, Shapiro E (2009) Molecular implementation of simple logic programs. Nat Nanotechnol 4(10):642–648
Ranallo S, Rossetti M, Plaxco KW, Vallée-Bélisle A, Ricci F (2015) A modular, DNA-based beacon for single-step fluorescence detection of antibodies and other proteins. Angew Chem 127(45):13412–13416
Ray SC, Bhunia SK, Saha A, Jana NR (2015) Graphene oxide (GO)/reduced-GO and their composite with conducting polymer nanostructure thin films for non-volatile memory device. Microelectron Eng 146:48–52
Rothemund PW (2005) Design of DNA origami. In: Proceedings of the 2005 IEEE/ACM international conference on computer-aided design, 2005. IEEE Computer Society, pp 471–478
Seeman NC (2010) Nanomaterials based on DNA. Annu Rev Biochem 79:65
Smijs TG, Pavel S (2011) Titanium dioxide and zinc oxide nanoparticles in sunscreens: focus on their safety and effectiveness. Nanotechnol Sci Appl 4:95
Song H, Zhang W, Cheng C, Tang Y, Luo L, Chen X, Luan C, Meng X, Zapien J, Wang N (2010) Controllable fabrication of three-dimensional radial ZnO nanowire/silicon microrod hybrid architectures. Cryst Growth Des 11(1):147–153

Song J, Lu H, Li S, Tan L, Gruverman A, Ducharme S (2015) Fabrication of ferroelectric polymer nanostructures on flexible substrates by soft-mold reverse nanoimprint lithography. Nanotechnology 27(1):015302
Su M, Li S, Dravid VP (2003) Microcantilever resonance-based DNA detection with nanoparticle probes. Appl Phys Lett 82(20):3562–3564
Sun T, Qiu J, Liang C (2008) Controllable fabrication and photocatalytic activity of ZnO nanobelt arrays. J Phys Chem C 112(3):715–721
Sun Y, Fuge GM, Ashfold MN (2004) Growth of aligned ZnO nanorod arrays by catalyst-free pulsed laser deposition methods. Chem Phys Lett 396(1):21–26
Sun Y, Fuge GM, Fox NA, Riley DJ, Ashfold MN (2005) Synthesis of aligned arrays of ultrathin ZnO nanotubes on a Si wafer coated with a thin ZnO film. Adv Mater 17(20):2477–2481
Sun Y, Kiang C-H (2005) DNA-based artificial nanostructures: Fabrication, properties, and applications. vol 2. American Scientific Publishers, Houston, TX
Tian ZR, Voigt JA, Liu J, Mckenzie B, Mcdermott MJ, Rodriguez MA, Konishi H, Xu H (2003) Complex and oriented ZnO nanostructures. Nat Mater 2(12):821–826
Vaseem M, Umar A, Hahn Y-B (2010) ZnO nanoparticles: growth, properties, and applications, vol 5. American Scientific Publishers, New York
Vayssieres L (2003) Growth of arrayed nanorods and nanowires of ZnO from aqueous solutions. Adv Mater 15(5):464–466
Venkataraman S, Dirks RM, Rothemund PW, Winfree E, Pierce NA (2007) An autonomous polymerization motor powered by DNA hybridization. Nat Nanotechnol 2(8):490–494
Wahab R, Kaushik NK, Verma AK, Mishra A, Hwang I, Yang Y-B, Shin H-S, Kim Y-S (2011) Fabrication and growth mechanism of ZnO nanostructures and their cytotoxic effect on human brain tumor U87, cervical cancer HeLa, and normal HEK cells. J Biol Inorg Chem 16(3):431–442
Wan M (2008) A template-free method towards conducting polymer nanostructures. Adv Mater 20 (15):2926–2932
Wang L, Sun Y, Li Z, Wu A, Wei G (2016) Bottom-up synthesis and sensor applications of biomimetic nanostructures. Materials 9(1):53
Wang X, Kong X, Yu Y, Zhang H (2007) Synthesis and characterization of water-soluble and bifunctional ZnO-Au nanocomposites. J Phys Chem C 111(10):3836–3841
Wang Y, Xia Y (2004) Bottom-up and top-down approaches to the synthesis of monodispersed spherical colloids of low melting-point metals. Nano Lett 4(10):2047–2050
Whitesides GM, Mathias JP, Seto CT (1991) Molecular self-assembly and nanochemistry: a chemical strategy for the synthesis of nanostructures. Science 254(5036):1312–1319
Wiradharma N, Zhang Y, Venkataraman S, Hedrick JL, Yang YY (2009) Self-assembled polymer nanostructures for delivery of anticancer therapeutics. Nano Today 4(4):302–317
Wu G, Xie T, Yuan X, Li Y, Yang L, Xiao Y, Zhang L (2005) Controlled synthesis of ZnO nanowires or nanotubes via sol–gel template process. Solid State Commun 134(7):485–489
Xia Y, Xiong Y, Lim B, Skrabalak SE (2009) Shape-controlled synthesis of metal nanocrystals: simple chemistry meets complex physics? Angew Chem Int Ed 48(1):60–103
Yan H, Park SH, Finkelstein G, Reif JH, LaBean TH (2003) DNA-templated self-assembly of protein arrays and highly conductive nanowires. Science 301(5641):1882–1884
Yang Y, Wu D, Han S, Hu P, Liu R (2013) Bottom-up fabrication of photoluminescent carbon dots with uniform morphology via a soft–hard template approach. Chem Commun 49 (43):4920–4922
Yao B, Chan Y, Wang N (2002) Formation of ZnO nanostructures by a simple way of thermal evaporation. Appl Phys Lett 81(4):757–759
Yin Z, Zheng Q (2012) Controlled synthesis and energy applications of one-dimensional conducting polymer nanostructures: an overview. Adv Energy Mater 2(2):179–218
Zhang B, Liu J, Guan S, Wan Y, Zhang Y, Chen R (2007) Synthesis of single-crystalline potassium-doped tungsten oxide nanosheets as high-sensitive gas sensors. J Alloys Compd 439 (1):55–58

Zhang J, Liu J, Peng Q, Wang X, Li Y (2006) Nearly monodisperse Cu_2O and CuO nanospheres: preparation and applications for sensitive gas sensors. Chem Mater 18(4):867–871
Zhang Q, Chou TP, Russo B, Jenekhe SA, Cao G (2008) Aggregation of ZnO nanocrystallites for high conversion efficiency in dye-sensitized solar cells. Angew Chem 120(13):2436–2440
Zhang Q, Dandeneau CS, Zhou X, Cao G (2009) ZnO nanostructures for dye-sensitized solar cells. Adv Mater 21(41):4087–4108